

## Nonenzymatic Glucose Sensor Based on Pt-Au-SWCNTs Nanocomposites

Xu Zhu, Chunlan Li, Xiaohua Zhu, Maotian Xu\*

Henan Key Laboratory Cultivation Base of Nanobiological Analytical Chemistry, Department of Chemistry, Shangqiu Normal University, Shangqiu 476000, People's Republic of China

\*E-mail: [xumaotian@sqnc.edu.cn](mailto:xumaotian@sqnc.edu.cn)

Received: 13 July 2012 / Accepted: 6 August 2012 / Published: 1 September 2012

---

A novel glucose nonenzymatic sensor is presented which is based on a glassy carbon electrode modified with Pt-Au nanocomposites (Pt-AuNCs) embedded in single-walled carbon nanotubes (SWCNTs). The Pt-Au nanocomposites were characterized using atoms force microscope (AFM) and electrochemistry methods, respectively. It can be found that most of Pt-AuNCs lie close to the texine of SWCNTs. Voltammetry was used to evaluate the electrocatalytic activities of the sensor toward nonenzymatic glucose oxidation in alkaline media. Under the optimal condition, the linear range for the detection of the glucose is 0.5–45mM with a correlation coefficient of 0.999, based on the oxidation peak observed during cathodic direction of the potential sweep. The kinetics and mechanism of glucose electro-oxidation were intensively investigated in this system. The sensor is also highly resistant toward poisoning by chloride ions and capable of sensing glucose oxidation in the presence of 0.05mM uric acid and 0.5mM ascorbic acid. This work provides a simple and easy approach to the detection of glucose in human serum with high sensitivity and excellent selectivity.

---

**Keywords:** glucose sensor; nonenzymatic; Pt-Au nanocomposites; single-walled carbon nanotubes; electrochemistry

### 1. INTRODUCTION

Glucose is a very useful component of animal and plant carbohydrates. Quantitative determination of glucose plays an important role in biochemistry, clinical chemistry, and food analysis [1, 2]. Recently, various techniques are presented for glucose analysis, such as infrared spectroscopy, Raman spectroscopy, photo acoustic spectroscopy, colorimetry, electrochemiluminescence and electrochemistry [3]. Due to their high accuracy, low cost, rapidity, simplicity and better detection limits, electrochemical sensors with and without glucose oxidase (GOx) have been proved to be powerful approaches and attracted much more attention [4]. The GOx-based glucose biosensor

catalyzes the oxidation of glucose to gluconolactone in the presence of oxygen, producing  $\text{H}_2\text{O}_2$  simultaneously [5-8]. Quantification of glucose is achieved via electrochemical oxidation of the liberated  $\text{H}_2\text{O}_2$ . Nevertheless, the oxidation of  $\text{H}_2\text{O}_2$  usually requires a relatively high positive potential (usually over +0.6 V vs. SCE) [9]. Many other electroactive species [10-13] commonly coexisting in the biological fluids, such as ascorbic acid (AA), uric acid (UA), can also be oxidized at such a high potential and their electrochemical signals, thus, severely affect the selectivity of the biosensors. The greatest drawback of these enzymatic glucose sensors is their lack of stability originating from the intrinsic nature of the enzymes, which is hard to overcome. The activity of these enzymes can also be easily affected by temperature, solution pH, humidity, and toxic chemicals. Although GOx is quite stable compared with other enzymes, GOx-based glucose sensors are always exposed to possible thermal and chemical deformation [14].

To address these issues, many attempts have been made to determine glucose without the use of enzymes. The majority of these nonenzymatic electrochemical glucose sensors rely on the current response of glucose oxidation directly at the electrode surface. Nowadays, numerous nanostructured materials have been reported, and their distinguishing characteristics certainly provide new opportunities for developing novel nonenzymatic glucose sensors [15, 16]. For instance, glucose detection has been reported using various nanomaterials as the nonenzymatic electrocatalysts. These nanomaterials include mesoporous Pt, nanoporous Au, Pd, Ni(II),  $\text{Cu}_2\text{O}$  nanowire arrays, and various alloys nanoarray [17-21].

Carbon nanotubes (CNTs) are unique one-dimensional materials with special mechanical and electronic properties and have been the focus of current research for many years. To optimize the use of CNTs in various applications, it is necessary to attach functional groups or other nanoparticles materials onto their surfaces [22]. The combination of CNTs with other nanocrystals is expected to be useful for catalysis, or making sensors. It is well known that CNTs are very hydrophobic and cannot be wetted by liquids due to their high surface tension, thus, most metals would not adhere to them. Surface modification and sensitization have been adopted attempting to improve metal deposition onto CNTs. One of the useful approaches is associated with the oxidation of the CNTs surface to create functional groups and increase metal nucleation [23]. However, the electrocatalytic activity of this catalyst is usually dropped onto the surface of the electrode, which will lead to more subjective factors.

Here we present a convenient and practical route for attachment of Pt-AuNCs on the SWCNT surfaces which involves covalent coupling of the activated SWCNTs subsequent protonization, and controllable assembly of Pt-AuNCs on the modified SWCNTs by deposition technique. A novel nonenzymatic glucose voltammetric sensor based on Pt-AuNCs/SWCNTs was then developed. The prepared sensor showed good analytical performance, indicating that the SWCNTs provided ample space to allow fast mass transport of ions through the electrolyte/electrode interface to obtain rapid electrochemical reactions, and Pt-AuNCs based devices exhibited good redox electrochemical activity and remarkably electrocatalytic activity for glucose.

## 2. EXPERIMENTAL

### 2.1. Materials and Reagents

Single-walled carbon nanotubes with carboxylic acid groups (SWCNTs–COOH, with a diameter of about 6nm and length of around 30 nm, purity >95%) were obtained from Chengdu Institute of Organic Chemistry, Chinese Academy of Sciences and used without further purification. Hydrogen tetrachloroaurate hydrate ( $\text{HAuCl}_4 \cdot 3\text{H}_2\text{O}$ ), Hydrogen hexachloroplatinic acid hydrate ( $\text{HPtCl}_4 \cdot 3\text{H}_2\text{O}$ ), AA, UA, and sodium dodecyl sulfate (SDS) were purchased from Alfa Aesar China Co., Ltd. (Tianjin, China). Glucose was purchased from Beijing Chemical Reagent (Beijing, China) and the stock solution was allowed to store at room temperature overnight before use. The supporting electrolyte was a 0.2 M NaOH solution. All other reagents were of analytical grade and used without further purification. All solutions were made up with ultrapure water (18.2 M $\Omega$ , Simplicity Plus, Millipore Corp.).

### 2.2. Instrumentations

Cyclic Voltammetry (CV), Amperometric i-t Curve (i-t), Multi-Potential Steps (STEP) and Linear Sweep Voltammetry (LSV) were performed on a CHI 660D electrochemistry work station (Shanghai CH Instrument Company, China). The three-electrode system consisted of a modified glassy carbon electrode or a bare glassy carbon electrode as a working electrode, a platinum electrode and a Ag/AgCl electrode were used as the auxiliary and reference electrodes, respectively. All potentials in this work are referenced to the Ag/AgCl. An atomic force microscope (Agilent 5500, Agilent Technologies, USA) was used to characterize the morphology of electrode in the presence or absence of SWCNTs and Au-PtNCs/SWCNTs.

### 2.3. Preparation of SWCNTs-COOH-GCE

Glassy carbon electrode (GCE, 3.0mm in diameter) was polished with 0.3 $\mu\text{m}$  and 0.05 $\mu\text{m}$  alumina slurry sequentially and then washed ultrasonically in ethanol and water for 5 minutes, respectively. After ultrasonical rinsing, the electrode was electrochemically pretreated by cyclic potential scanning between  $\pm 1.0$  V in 0.02 M  $\text{H}_2\text{SO}_4$  until cyclic voltammogram of clean GCE was obtained. Afterwards, clean electrode was immersed in 0.2 mg mL<sup>-1</sup> solutions ( The acid pretreated SWCNTs were then dispersed into 0.1% (wt %) SDS solution in an ultrasonic bath to prepare an aqueous suspension of SWCNTs with a loading of 0.2 mg mL<sup>-1</sup> ). The target GCE was connected as the positive pole whereas a platinum electrode was used as the negative pole. A potential of 10V (DC) was applied for 30s electrophoretic accumulation of acid pretreated SWCNTs. It can be seen that the GCE was covered with a blue thin film.

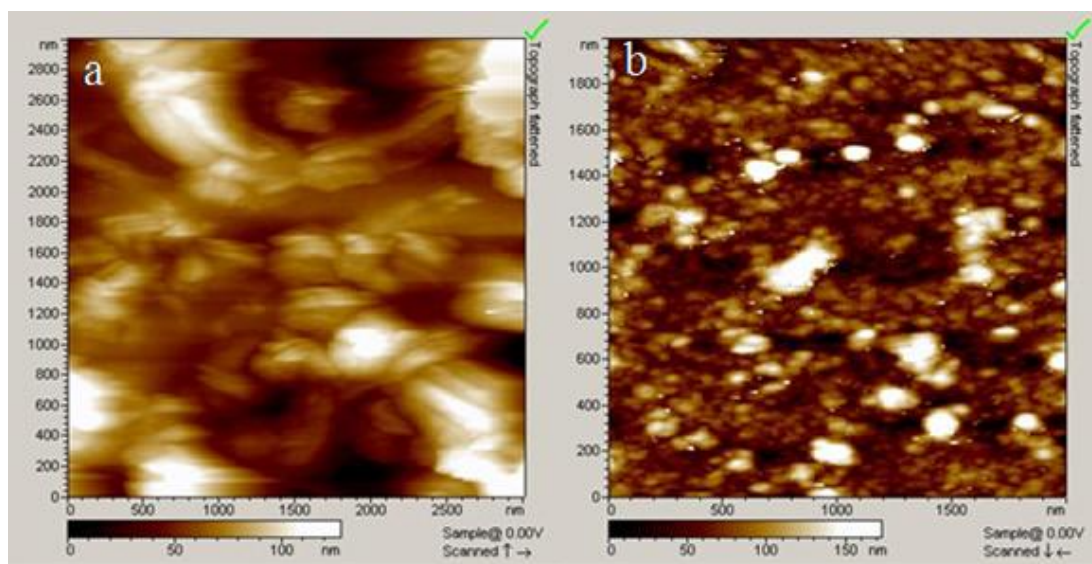
#### 2.4. Synthesis of Pt and Au nanoparticles

After the electrode was dried, immerse the SWCNTs/GCE into a 10 mM HPtCl<sub>4</sub> solution 2 min to entire surface and pore walls of the membrane and carefully dried through nitrogen. After that, the electrode was immersed in HAuCl<sub>4</sub> solution (1mM). A technique of multi-potential steps was employed for the direct electrodeposition of Pt-Au nanocomposites. In a first series of experiments, a pulse potential profile of 200 mV (500 ms) ~ -1200 mV (100 ms) ~200 mV (500 ms) (vs. Ag/AgCl 3M KCl) was applied and 45 pulses were used for each deposition. In this way, a rather high loading of Pt-Au nanocomposites on the carbon nanotubes could be achieved. At the end of each assembly process, the modified electrode was thoroughly washed with pure water. It was observed that the GCE was covered with a golden-black thin film. The modification process above was confirmed by AFM and CV techniques.

### 3. RESULTS AND DISCUSSION

#### 3.1. Morphology of the multilayer films

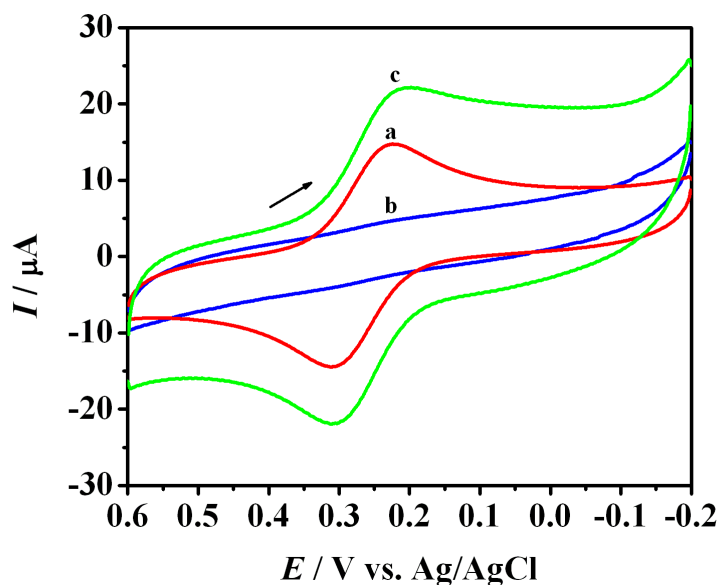
Direct morphological observation of the as-prepared Au-PtNCs/SWCNTs modified electrode was made using an AFM. The typical AFM images are shown in Fig.1.



**Figure 1.** AFM images of the surface morphology of (a) SWCNTs/GCE and (b) Au-PtNCs/SWCNTs/GCE.

Fig.1a shows the AFM image of the surface of SWCNTs/GCE. It can be seen that the diameters of SWCNTs is in range from 5 to 10 nm. Fig.1b gives a representative AFM image of the surface of Au-PtNCs/SWCNTs/GCE in which many Au-Pt dots grown on the SWCNTs with a higher

density of hydroxyl groups can be seen. In addition, the (Pt-AuNCs/SWCNTs) films were homogeneous with well dispersed Pt-Au nanoparticles.



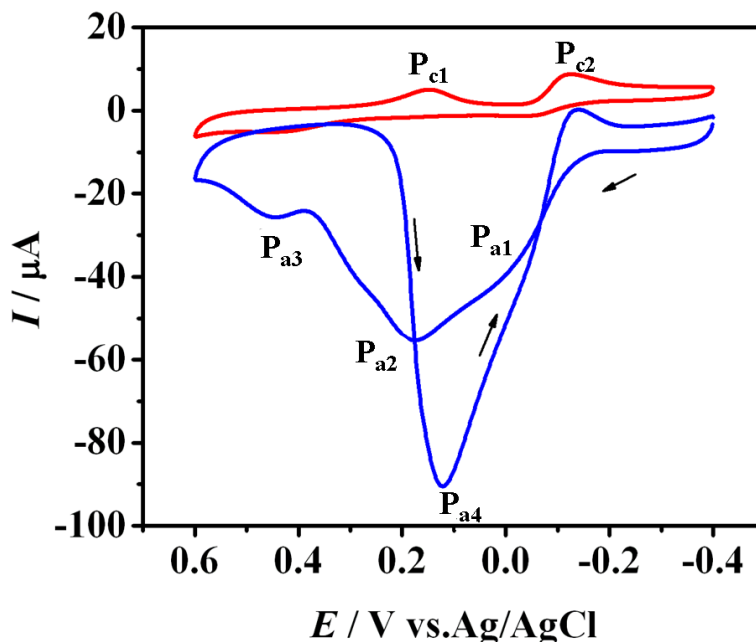
**Figure 2.** Cyclic voltammetry of 10mM  $K_3[Fe(CN)_6]$  in 0.1M KCl solutions at 100 mV/s for (a) bare GCE, (b) SWNTs/GCE and (c) Pt-AuNCs/SWCNTs/GCE. The scan rate was 100 mV/s.

Fig.2 shows the cyclic voltammetry (CV) response for different electrodes in 0.1M KCl solution containing 10mM  $K_3[Fe(CN)_6]$  at 100mV/s. Redox reactions easily occurred on a bare GCE, evidenced by very large redox currents. After the substrate has been covered a layer of SWCNTs, the CV curve dramatically changes from an electrochemically reversible shape to a capacitive shape. Electrode modified with Pt-AuNCs/SWCNTs hybrids exhibited a pair of larger and reversible cathodic/anodic peaks of  $[Fe(CN)_6]^{3-/4-}$ . Compared with the bare GCE, the bigger peak-to-peak separation ( $\Delta E_p$ ) seems to indicate slow kinetics between the electrodes. But the fact which is responsible for the above phenomena may be explained by the strong electron-blocking effect of layer between Pt-Au NPs and the bare GCE.

### 3.2. Electrocatalytic oxidation of glucose

The cyclic voltammograms (CV) method was used to compare and investigate the catalytic activity of the as-prepared Pt-AuNCs/SWCNTs modified electrode. As shown in Fig. 3, the CV curve of Pt-AuNCs/SWCNTs modified electrode measured in 0.2M NaOH demonstrates typical Pt-Au oxidation/reduction behavior usually associated to formation and reduction of Pt-Au oxide [24], which corresponds to  $P_{c1}$  at 0.148 V ( red curve) and  $P_{a3}$  at 0.451 V ( blue curve). The current decreased at a higher applied potential owing to the evolution of oxygen on the Pt-Au surface, and oxygen covered the active sites. The observed large electrochemical response of the Pt-AuNCs/SWCNTs modified electrode is due to the significantly enhanced effective surface area and improved electrocatalytic

activity. In the presence of glucose, two more oxidation peaks ( $P_{a1}$  at  $-0.028\text{V}$  and  $P_{a2}$  at  $0.175\text{V}$ , blue curve) appear in the anodic potential sweep together with a much more pronounced glucose oxidation peak appear at  $0.121\text{V}$  ( $P_{a4}$ , blue curve) during the potential sweep in the cathodic direction. Obviously, this peak is overlapped with the reduction peak of Pt-Au oxide ( $P_{c1}$ ).



**Figure 3.** CV curves at the Pt-AuNCs/SWCNTs/GCE in 0.2M NaOH solution with (blue) and without (red) 5mM glucose. The scan rate was 20 mV/s.

The peak currents of  $P_a$  increase linearly with the square root of the scan rate in the range of 0.01-0.6 V/s. After washing the electrode with a large amount of ultrapure water and afterwards putting it in a blank solution (0.2 M NaOH), no oxidation peak appears in the negative potential sweep (data not shown). These results show that glucose is hardly adsorbed at the surface of Pt-AuNCs/SWCNTs modified electrode and the electrode reaction is controlled by the diffusion of glucose in the solution. Meanwhile, this also indicates that the faradic response of a sluggish reaction like glucose oxidation would be significantly improved by the Pt-AuNCs. On the other hand, the peak potential of  $P_{a4}$  is affected strongly by the reduction peak potential of Pt-Au oxide ( $P_{c1}$ ). It is reasonable that the peak potential of  $P_{c1}$  is followed by  $P_{a4}$  as the oxidation of glucose is based on free Pt-AuNCs. With the increase of potential scan rate, both the peak potentials of  $P_{a4}$  and  $P_{c1}$  move to more negative values, while the peak current of  $P_{a4}$  first increases and then decreases after its peak potential below 0 V. It can be explained by the fact that when the potential is below 0V, the second oxidation of glucose corresponding to  $P_{a1}$  would not occur, hence low peak current would be observed. It should be pointed out that the catalytic peak here was only obtained at higher concentrations of glucose ( $>0.1\text{mM}$ ) and could not be observed in the micromolar range.

### 3.3. Voltammetric detection of glucose

There are many reports regarding amperometric sensing applications of glucose by measuring current response at a fixed potential and within a certain time after adding the analyte and possible interfering species [25-27]. In this paper, voltammetric response of Pt-AuNCs/SWCNTs/GCE in 0.2M NaOH solution has been regarded as the optimal mode for the high-sensitivity detection of glucose in body fluid. To improve the performance of the glucose sensor, several factors such as the NaOH concentrations were optimized. In the alkaline solution, Au played its catalytic role efficiently. This deduction could be further confirmed from CV result of the glucose solution containing 0.2M PBS (pH=7.4) and  $\text{NH}_3\text{-NH}_4\text{Cl}$  (pH=10.0) where no obvious catalytic peak could be found in the CV curve (data not shown), which indicates that  $\text{OH}^-$  plays an important role in glucose oxidation on the Pt-AuNCs/SWCNTs modified electrode. Although higher concentration of  $\text{OH}^-$  in the solution caused higher electrocatalytic activity of Au, on the contrary, too much  $\text{OH}^-$  blocked the further electroadsorption of glucose anion, resulting in decrease in current. As a result, 0.2M NaOH was selected for the electrocatalytic oxidation of glucose.

We further investigated the peak currents in glucose sensing with different ratios between SWCNTs and Au on Pt-AuNCs/SWCNTs modified electrode at the above result. As shown in Fig. 4, the peak current increased with increasing cycles from 20 to 45 and decreases above 45 cycles. The test results showed that the maximum current response occurred at 45 cycles. Thus, 45 cycles were chosen for the multi-potential steps electrodeposition throughout this study.

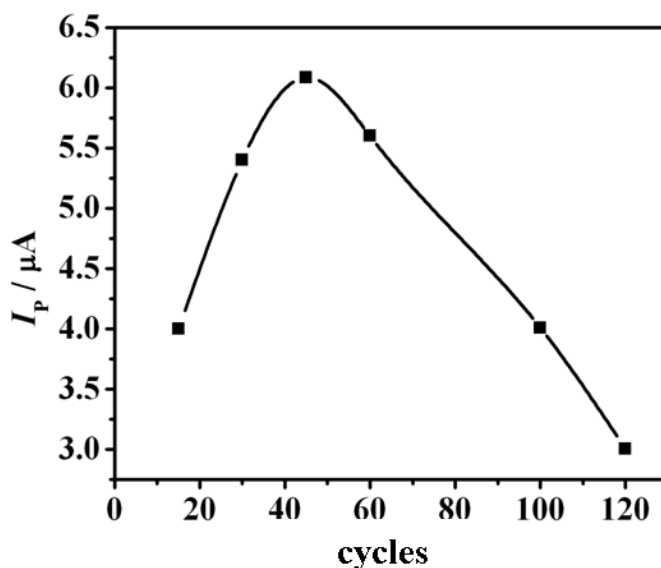


**Figure 4.** The relationship between peak current and the cycles of multi-potential steps electrodeposition.

Based on the above result, successive addition of 50  $\mu\text{L}$  1.0M glucose (final volume 10.0mL) to the solution was performed. Upon addition of glucose at regular intervals, rapid increase in currents

was observed. The proposed biosensor presents a linear response to glucose concentration within the range from 0.5 mM to 45mM ( $r=0.999$ ), as presented in Fig. 5. It also provides a very low detection limit of 0.1 mM estimated at a signal-to-noise ratio of 3.

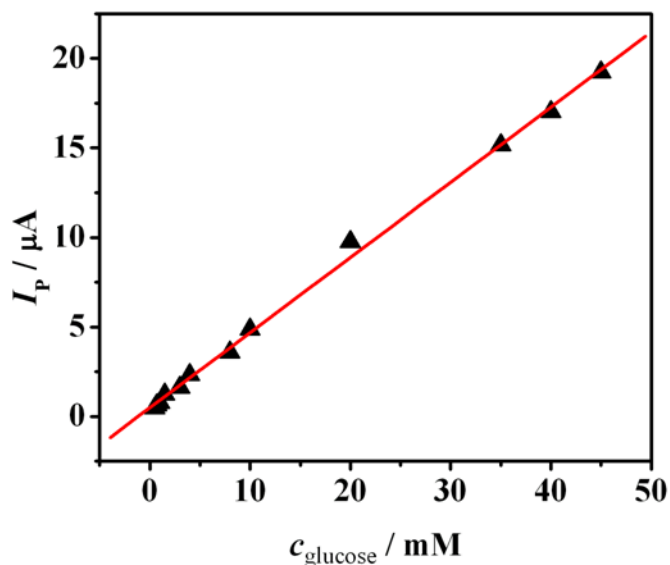


**Figure 5.** Calibration curve of the peak current of the biosensor to glucose concentration in 0.2M NaOH. (Inset) The linear part of the calibration curve.

### 3.4. Elimination of interfering substance

As mentioned in the introduction, one of the major challenges in nonenzymatic glucose detection is the interfering electrochemical signals caused by some easily oxidizable compounds such as AA and UA. In order to verify the performance of this nonenzymatic glucose voltammetric sensor based on Pt-AuNCs/SWCNTs modified electrode, some possible interfering species such as AA, UA and  $\text{Cl}^-$  were added into sample solution. In the evaluation of an amperometric sensor, current responses were measured under different concentrations of the objective analyte at a fixed potential and at fixed times [28]. The Pt-AuNCs/SWCNTs modified electrode can be successfully used to detect glucose without any interference in the existence of 0.05mM UA and 0.5mM AA (data not shown), which may attribute to the significantly enhanced effective surface area and the improved catalytic activity of the Pt-AuNCs/SWCNTs/GCE.

Most electrochemical glucose sensors based on metals or alloys are easy to lose their activity due to the poisoning effect of chloride ions [29, 30]. In order to understand whether chloride ions poison the electrocatalytic ability of the Pt-AuNCs/SWCNTs modified electrode for glucose oxidation, we studied the amperometric responses in solution containing various concentrations of KCl. It has been reported that in the presence of  $\text{Cl}^-$ , part of the surface-active sites could be preferentially blocked, causing less chance of reactive species approaching the electrode surface. However, in our experiment, the Pt-AuNCs/SWCNTs modified electrode could still make a rather strong and stable current signal even in a concentration of 0.2 M  $\text{Cl}^-$ , which is larger than the physiological value (0.16



M) (data not shown). Although this phenomenon was also reported by other researchers, its mechanism is still unclear. In the modified electrode, the negatively charged Pt-AuNCs may be useful to prevent the nanoparticles from being poisoned by  $\text{Cl}^-$  in alkaline solution, thus, it can be helpful in resisting poisoning by  $\text{Cl}^-$ .

### 3.5. Stability

The stability was investigated by using the same Pt-AuNCs/SWCNTs modified electrode for voltammetric measurement of 5 mM glucose in 0.2M NaOH solution and recording the peak current for the oxidation of glucose at regular intervals (every 3 h) over 72 h. Before each measurement, the electrode was electrochemically cleaned in 0.2 M NaOH solution. It was found that the magnitude of each peak current exhibits only slight change from one another and 93% of the original response remains after 24 measurements. An identical experiment was carried out at another Pt-AuNCs/SWCNTs modified electrode and no obvious difference was shown. These experiments show that the Pt-AuNCs/SWCNTs modified electrode is stable and can be used for repeated measurements of glucose.

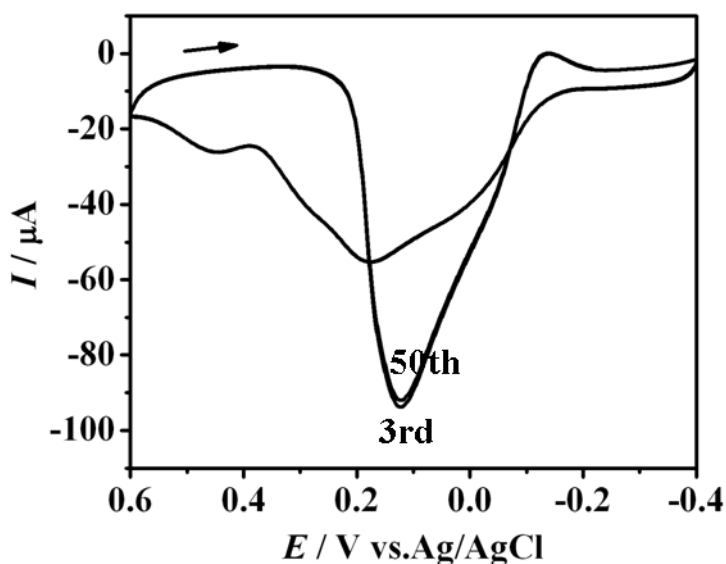


**Figure 6.** Stability of the cyclic voltammetric features of the Pt-AuNCs/SWCNTs/GCE in 0.2M NaOH solution containing 5 mM glucose on the continuously scanning (the 3rd and the 50th cycles). The scan rate was 20mV/s.

Furthermore, the electrocatalytic characteristics of the Pt-AuNCs/SWCNTs modified electrode catalyst toward the oxidation of glucose are fairly stable since the features of the cyclic voltammograms remained invariable after the Pt-AuNCs/SWCNTs modified electrode was scanned continuously in NaOH solution containing 5 mM glucose for 50 cycles (Fig.6). Therefore, the Pt-

AuNCs/SWCNTs have acceptable stability in the potential range where they are used as an electrocatalyst for the oxidation of glucose.

### 3.6. Determination of glucose in real samples

In order to evaluate the applicability of the proposed method to the determination of glucose in real samples, the utility of the developed method was tested by determining glucose in human serum sample. The results are summarized in Table 1. The good recoveries of the mixture samples indicate the successful applicability of the proposed method to determination of glucose.

**Table 1.** Detection results of glucose in human serum samples.

NO.	Glucose Spiked (mM)	Glucose Found (mM)	Recovery (%)
1	-	5.5	-
2	5.0	10.6	102
3	10.0	15.8	103
4	20.0	26.1	103

## 4. CONCLUSIONS

In summary, a quick, simple and sensitive electrochemical biosensor has been developed for glucose detection based on the application of such a novel nanocomposite consisting of Au, Pt and SWCNTs. Pt-AuNCs show good electrocatalytic activity to glucose oxidation at the cathodic direction of the potential sweep, owing to some synergistic effects among Pt-AuNCs and SWCNTs. The simplicity, stability and durability make the modified electrode a very good platform for biosensors.

## ACKNOWLEDGEMENTS

The authors greatly appreciate the supports of the National Natural Science Foundation of China (Nos. 21045003 and 21175091).

## References

1. K. Wang, J. Xu, D. Sun, H. Wei and X. Xia, *Biosens. Bioelectron.*, 20 (2005) 1366.
2. S. Kang, R. Jeong, S. Park, T. Chung, S. Park and H. Kim, *Anal. Sci.*, 19 (2003) 1481.
3. A. Heller and B. Feldman, *Chem. Rev.* 108 (2008) 2482.
4. H. Wang, X. Wang, X. Zhang, X. Qin, Z. Zhao, Z. Miao, N. Huang and Q. Chen, *Biosens. Bioelectron.*, 25 (2009) 142.
5. J. Du, X. Yu and J. Di, *Biosens. Bioelectron.*, 37 (2012) 88.
6. Y. Yan, R. Tel-Vered, O. Yehezkeli, Z. Cheglakov and I. Willner, *Adv. Mater.* 20 (2008) 2365.
7. Z. Wang, S. Liu, P. Wu and C. Cai, *Anal. Chem.* 81 (2009) 1638.
8. F. Xiao, F. Zhao, Y. Zhang, G. Guo and B. Zeng, *J. Phys. Chem. C* 113 (2009) 849.

9. J. Chen, J. Bao, C. Cai and T. Lu, *Anal. Chim. Acta.*, 516 (2004) 29.
10. S. Liu, C. Cai and J. Xu. *Electroanal. Chem.*, 602 (2007) 103.
11. C. Chou, J. Chen, C. Tai, W. Sun and J. Zen, *Electroanalysis*, 20 (2008) 771.
12. B. Fang, C. Zhang, G. Wang, M. Wang and Y. Ji, *Sens. Actuators B: Chem.*, 155 (2011) 304.
13. M. Tominaga, T. Shimazoe, M. Nagashima and I. Taniguchi, *Chem. Lett.*, 34 (2005) 202.
14. L. Meng, J. Yang, T. Lu, H. Zhang and C.X. Cai, *Anal. Chem.*, 81 (2009) 7271.
15. Y. Bai, W. Yang, Y. Sun and C. Sun, *Sens. Actuators B: Chem.*, 134 (2008) 471.
16. S. Cho and C. Kang, *Electroanalysis*, 19 (2007), 2315.
17. S. Park, T. Chung and H. Kim, *Anal. Chem.*, 75 (2003) 3046.
18. L. Rong, C. Yang, Q. Qian and X. Xia, *Talanta*, 72 (2007) 819.
19. Y. Song, D. Zhang, W. Gao and X. Xia, *Chem. Eur. J.*, 11 (2005) 2177.
20. J. Ye, Y. Wen, W. Zhang, L. Gan, G. Xu and F. Shen, *Electrochem. Commun.*, 6 (2004) 66.
21. Y. Li, Y. Song, C. Yang and X. Xia, *Electrochem. Commun.*, 9 (2007) 981.
22. M. Tominaga, T. Shimazoe, M. Nagashima and I. Taniguchi, *Electrochem. Commun.*, 7 (2005) 189.
23. J. Wang, X. Sun, X. Cai, Y. Lei, L. Song and S. Xie, *Electrochem. Solid State Lett.*, 10 (2007) J58.
24. F. Kurniawan, V. Tsakova and V. M. Mirsky, *Electroanalysis*, 18 (2006) 1937.
25. Y. Song, Z. Gao, K. Lee and P. Shmuki, *Electrochem. Commun.*, 13 (2011) 1217.
26. J. H. Shim, K. Jiang, C. Lee and Y. Lee, *Electroanalysis*, 23 (2011) 2063.
27. J. Ryu, K. Kim, H. Kim, H. T. Hahn and D. Lashmore, *Biosens. Bioelectron.*, 26 (2010) 602.
28. D. W. Kimmel, G. LeBlanc, M. E. Meschievitz and D. E. Cliffel, *Anal. Chem.*, 84 (2012) 685.
29. J. Wang, D. F. Thomas and A. Chen, *Anal. Chem.*, 80 (2008) 997.
30. C. Su, C. Zhang, G. Lu and C. Ma, *Electroanalysis*, 22 (2010) 1901.